

Environment-Aware and Human-Cooperative Swing Control for Lower-Limb Prostheses in Diverse Obstacle Scenarios

Haosen Xing, Haoran Ma, Sijin Zhang, and Hartmut Geyer

Abstract—Current control strategies for powered lower limb prostheses often lack awareness of the environment and the user’s intended interactions with it. This limitation becomes particularly apparent in complex terrains. Obstacle negotiation, a critical scenario exemplifying such challenges, requires both real-time perception of obstacle geometry and responsiveness to user intention about when and where to step over or onto, to dynamically adjust swing trajectories. We propose a novel control strategy that fuses environmental awareness and human cooperativeness: an on-board depth camera detects obstacles ahead of swing phase, prompting an elevated early-swing trajectory to ensure clearance, while late-swing control defers to natural biomechanical cues from the user. This approach enables intuitive stepping strategies without requiring unnatural movement patterns. Experiments with three non-amputee participants demonstrated 100% success across more than 150 step-overs and 30 step-ons with randomly placed obstacles of varying heights (4-16 cm) and distances (15-70 cm). By effectively addressing obstacle navigation—a gateway challenge for complex terrain mobility—our system demonstrates adaptability to both environmental constraints and user intentions, with promising applications across diverse locomotion scenarios.

I. INTRODUCTION

The ability of lower-limb assistive devices to function effectively is challenged by the unpredictability of real world environments. Although several approaches to the control of lower limb prostheses and exoskeletons have been developed [1]–[7], these approaches often struggle to adapt to complex scenarios such as obstacle crossings due to their reliance on pre-programmed motion patterns. Consequently, incorporating environmental information into control has become a promising research direction [8] with the potential for lower-limb assistive devices to detect and respond to changes in the environment in real time and therefore to provide safer and more comfortable use [9].

Research on integrating such environmental information has focused primarily on terrain recognition and classification. This involves using sensors such as laser scanners [10], [11], depth cameras [12]–[19], and RGB cameras [20]–[25] to capture and classify the terrain ahead of a user with the goal of adjusting the pre-programmed motion patterns of assistive devices in anticipation of the upcoming environment. However, relying solely on classification has drawbacks. Even with reported classification accuracies ranging from 82% to

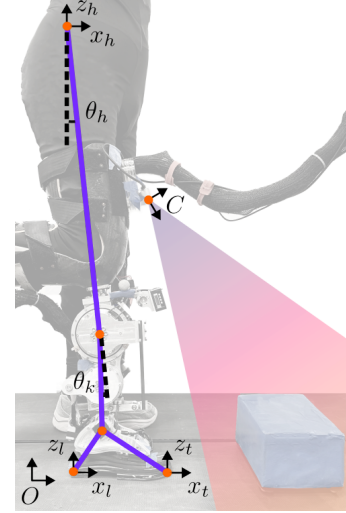


Fig. 1. Powered knee and ankle prosthesis with depth camera mounted on able-bodied adapter. Kinematic model of user and prosthesis for state estimation and control shown in blue with world (O) and camera (C) coordinate frames, user hip angle (θ_h , relative to world frame vertical) and position (x_h, z_h), and prosthetic knee angle (θ_k) and toe (x_t, z_t) and heel (x_l, z_l) positions highlighted.

99%, this would still translate into 3 to 54 falls per month [9]. Furthermore, terrains classified with the same label can vary widely in size and shape, demanding additional refinement in control strategies to effectively mitigate fall risks.

With a focus on lower limb prostheses, recent studies have started to include more detailed information about the environment in the control design. For instance, [26] and [27] incorporate the distance and height of detected obstacles to re-plan the motion of a lower limb prosthesis for the upcoming swing phase. These approaches, however, do not account for the user’s intended decision, such as the desire to modify the limb motion *during* the swing phase. Toward a more flexible prosthesis behavior with human intent integrated, [28] presented a swing controller for stepping over obstacles by continuously modifying the joint velocities of the prosthesis based on its current distance to the obstacle, while the user’s thigh motion determined the height of the foot during the step-over. Similarly, [29] presented a reactive controller that adapts the motion of the prosthesis throughout swing using estimates of the pose of the prosthesis and of the future path of the user’s hip to avoid scuffing the ground and tripping. Nonetheless, both studies predefined the position of the prosthesis at the end

H. Xing, H. Ma, S. Zhang, and H. Geyer are with the Robotics Institute, Carnegie Mellon University, Pittsburgh, PA 15213, USA. {haosenx, sijinz, hgeyer}@andrew.cmu.edu, haoram98@gmail.com.

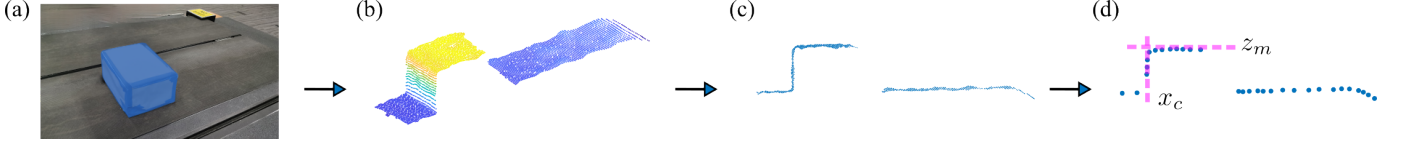


Fig. 2. Processing steps for extracting environment information. (a) Example of obstacle encounter on the treadmill. (b) Corresponding 3-D point cloud cropped to a width of 15 cm to reduce data processing. (c) Point cloud projected onto sagittal plane. (d) Pruned elevation map with identified maximum obstacle height (z_m) and horizontal distance from the toe location to the (projected) front of the obstacle (x_c).

of the swing, severely limiting the flexibility of the controller. For example, rather than to step over an obstacle, a user might want to step onto it. An ideal human assistive device should seamlessly integrate such user preferences into the device control [30].

Here, we present a more human-cooperative prosthesis control that adapts the swing motion of the prosthesis dynamically in response to environmental information and includes the user in making decisions about where and when to land. To this end, we integrate computer vision and state estimation algorithms to create a swing controller that synchronizes the prosthesis's knee motion with the user's estimated hip motion, yet continually adapts this synchronization based on information about obstacles in the path of the prosthesis. By not predefining the final position of the prosthesis, the user maintains authority over where and when landing occurs. We then demonstrate the effectiveness of the proposed control in experiments with three non-amputee participants who use the powered knee and ankle prosthesis with an adapter (Fig. 1) during level walking and when stepping over and onto obstacles of various sizes and distances at the onset of swing. Finally, we discuss the potential of the proposed control to not only allow flexible obstacle negotiation but also generalize to locomotion in any environment.

II. SWING CONTROL

A. Environment Information

We extract environment information from a depth camera (Intel RealSense D435) mounted on the able-bodied adapter of the knee and ankle prosthesis (Fig. 1). The camera generates a 3-D point cloud of the terrain ahead of the prosthesis, which we capture during the late stance phase when the camera points downward (Fig. 2-a,b). We transform the point cloud into the global coordinate frame O using state estimation based on two IMUs on the prosthesis (mounted above the knee and on the foot) and project it onto the sagittal plane (Fig. 2-c). We then prune this projection using K-means clustering [31] for key point detection, resulting in an elevation map from which we extract the maximum elevation z'_m and the horizontal distance x_c from the prosthesis toe to the largest elevation change (Fig. 2-d).

For control purposes, we modify the two estimates. First, we modify the elevation estimate to the obstacle height $z_m = \max(z'_m, z_t) + \delta$, where z_t is the prosthesis toe height in late stance and $\delta = 1$ cm. Besides introducing a safety margin, this modification ensures that the prosthesis foot lifts off the ground in level walking and when encountering lowering elevation profiles (such as in stair and ramp declines, not

investigated here). Second, if indeed $z'_m \leq z_t$, we set x_c to the arbitrary value of 20 cm, which leads to a satisfactory lift-off trajectory of the prosthesis in level walking.

B. Prosthesis Knee Swing Controller

For controlling the prosthesis motion during swing, we assume that the foot remains perpendicular to the shank throughout the swing and model the prosthesis as a two-link manipulator with hip and knee joints (θ_h and θ_k). The controller uses this model to plan the desired knee velocity of the prosthesis based on the current motion of the user's hip and on the height z_m and distance x_c of the obstacle extracted from the elevation map. More specifically, planning occurs in the joint space, where the current pose of the prosthesis reduces to a point $\mathbf{P}(\theta_h, \theta_k)$ and obstacle information defines forbidden areas that change over time [32]. The planning uses estimates of the hip, toe and heel locations of the prosthesis (O -frame coordinates x_h, z_h, x_t, z_t, x_l and z_l) and of the angles and angular velocities of the hip and knee ($\dot{\theta}_h, \dot{\theta}_k$) and the knee angular acceleration ($\ddot{\theta}_k$) (details on state estimation in a recent work [citation omitted for anonymity]) (Fig. 1). Planning is divided into three phases.

1) *Phase One—Raise Toe Above Obstacle Height*: The goal of phase one is to raise the prosthesis toe above the obstacle height z_m before x_t reaches the location x_c . To achieve this goal, we consider two regions of the joint space shown in figure 3-b. The first region, M_x^t , marks all joint configurations in which the toe has not yet reached the obstacle, $x_t < x_c$ (light blue). The second, M_z^t , represents joint configurations with the toe below the estimated obstacle height, $z_t < z_m$ (red). The superscript t indicates that these regions change dynamically; for example, as the user moves forward and elevates the hip, M_x^t shifts leftward and M_z^t shrinks. Due to the shift to the left, the joint configuration \mathbf{P}^t of the prosthesis will exit M_x^t eventually, and successful control in phase one requires \mathbf{P}^t to exit M_z^t beforehand, as the latter becomes a forbidden region once $x_t \geq x_c$. Given an initial configuration \mathbf{P}^0 , the correct exit order can be achieved by moving along the slope $k_1^t = \frac{\Delta\theta_k^t}{\Delta\theta_h^t}$, where $\Delta\theta_k^t$ is the vertical distance to the edge of M_z^t and $\Delta\theta_h^t$ is the horizontal distance to the edge of M_x^t . Thus, in phase one, we set the desired knee angular velocity $\dot{\theta}_k^{t+1}$ of the prosthesis for the next time step ($t+1$) to

$$\dot{\theta}_k^{t+1} = k_1^t \dot{\theta}_h^t, \quad (1)$$

where $\dot{\theta}_h^t$ is the estimated hip angular velocity of the user. Note that if an obstacle detected by the camera is very far away, the region M_x^t may expand far to the right of the configuration

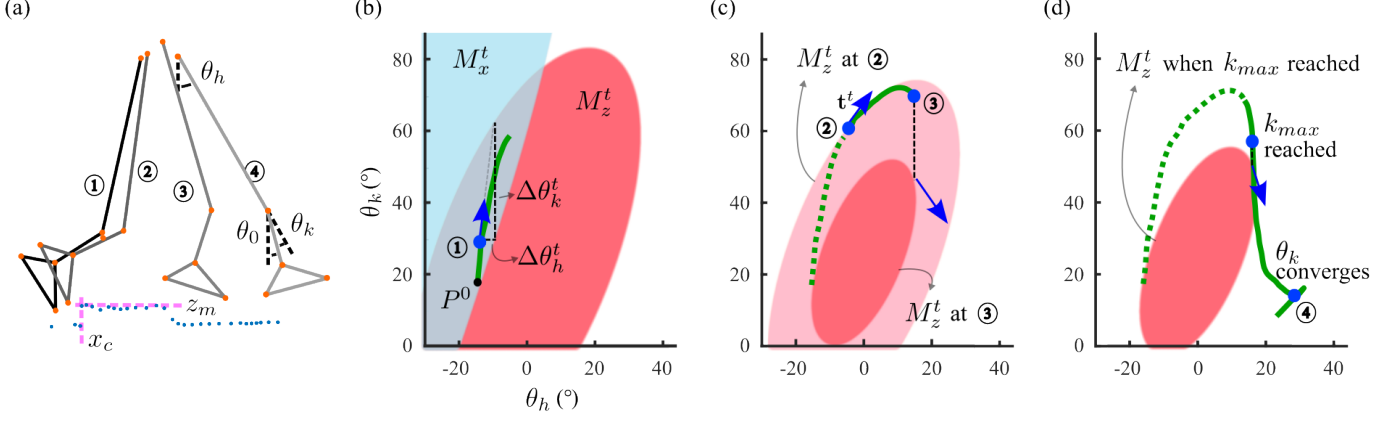


Fig. 3. Swing control overview. (a) Elevation map and kinematic model at start of swing (1), transitions to phase two (2) and three (3), and when the knee angle starts to mirror the hip angle in phase three (4). (b) Phase one with example of current regions of joint configurations for which prosthesis toe has not yet reached obstacle (M_x^t , light blue) and for which the toe is below the obstacle height (M_z^t , red). Also shown are generated trajectory from initial configuration P^0 with configuration corresponding to kinematic model (1) marked as blue point. Dashed lines indicate horizontal and vertical distances of hip ($\Delta\theta_h^t$) and knee angle ($\Delta\theta_k^t$) to region boundaries (c) Phase two with forbidden region M_z^t at beginning (light red) and end (red) of the phase. Blue arrows show respective tangents \mathbf{t}^t of region boundary at current hip angle. (d) Phase three with forbidden region at moment when magnitude of slope reaches k_{max} (compare text) and trajectory of \mathbf{P}^t until the touchdown. Once the knee angle has converged to $\theta_k^t = \theta_h^t - \theta_0$ (4), changes in the knee angle strictly mirror changes in the hip angle and the prosthesis shank maintains a constant forward lean θ_0 in preparation for landing (see panel (a)).

space and the vertical distance $\Delta\theta_k^t$ cannot be established. To ensure fast enough lift off in this case, we enforce a lower threshold $k_1^t \geq k_{min}^t$, where k_{min}^t corresponds to the slope obtained assuming that $\Delta\theta_k^t$ is the vertical distance between the current point \mathbf{P}^t and the peak of the region M_z^t .

2) *Phase Two—Maintain Toe Height*: Once the toe height of the prosthesis reaches the obstacle height, the control switches to phase two with the goal of maintaining z_t above z_m . One way to achieve this goal is to strictly follow the contour of the forbidden region M_z^t in the joint space. However, such a strict policy leads to unnecessarily aggressive prosthesis behavior, as M_z^t tends to shrink rapidly due to hip elevation by the human user. Instead, we rely on the tangent vector \mathbf{t}^t of the contour (Fig. 3-c), which varies much less rapidly and generates a smoother prosthesis behavior. Specifically, we set the desired knee angular velocity to the instantaneous slope k_2^t of the tangent vector,

$$\dot{\theta}_k^{t+1} = k_2^t \dot{\theta}_h^t. \quad (2)$$

Note that when $k_2^t < 0$, M_z^t remains unchanged to ensure further smoothness and prevent potential M_z^t inflation.

3) *Phase Three—Prepare For Landing*: Once the horizontal position of the heel passes that of the hip, $x_l > x_h$, the control switches to phase three. In this phase, the swing leg points forward, and the goal is to extend the knee and prepare the leg for landing regardless of whether the user intends to step onto or over the obstacle. The extension happens largely automatically by continuing to set the desired angular velocity of the knee according to (2), as the slope of the tangent of M_z^t is negative when the heel has passed the hip position (compare Fig. 3-c). However, we introduce a few practical tweaks. First, since the hip velocity can sometimes go to zero, we use its iterative maximum, $\dot{\theta}_h^t = \max_{\tau} \dot{\theta}_h^{\tau}$ to prevent freezing of the knee, where τ goes from the start time of phase three to the current time. Second, because the tangent will inevitably point

straight down at some point in this phase (Fig. 3-c), we prevent excessive knee velocities by saturating the magnitude of the slope to k_{max} . Third, once the slope reaches this saturation level, we switch the control to

$$\dot{\theta}_k^{t+1} = C^t k_{max} \dot{\theta}_h^t \quad (3)$$

with

$$C^t = \frac{\theta_k^t - \theta_h^t + \theta_0}{\theta_k^* - \theta_h^* + \theta_0}, \quad (4)$$

where the term C^t ensures the knee converges to an angle $\theta_k^t = \theta_h^t - \theta_0$ that is offset from the hip angle by θ_0 , and θ_k^* and θ_h^* are the knee and hip angles at the time when the slope reached the saturation level. Finally, once the knee angle has converged, we apply

$$\dot{\theta}_k^{t+1} = \dot{\theta}_h^t, \quad (5)$$

and the prosthesis shank maintains the same pose (forward lean by offset angle θ_0 with respect to the world frame vertical) in preparation for landing until the prosthesis foot detects contact. (The parameters θ_0 and k_{max} are hand-tuned.)

4) *Phase transitions*: To ensure smooth prosthesis motions, the velocity command sent to the prosthesis knee gradually transitions at the beginning of a new phase,

$$\dot{\theta}_{k,cmd}^{t+1} = (1 - \gamma_1) \dot{\theta}_k^{t+1} + \gamma_1 \left(\dot{\theta}_{k,msd}^t + \gamma_2 \ddot{\theta}_{k,ini}^t \Delta t \right), \quad (6)$$

where $\dot{\theta}_{k,msd}^t$ is the measured prosthesis knee velocity, $\ddot{\theta}_{k,ini}^t$ is the knee acceleration at the start of the new phase, Δt is the controller time step, and $\gamma_i = e^{-\alpha_i n}$ are exponential decay terms defined by tuning parameters α_i and the number n of time steps since the start of the new phase.

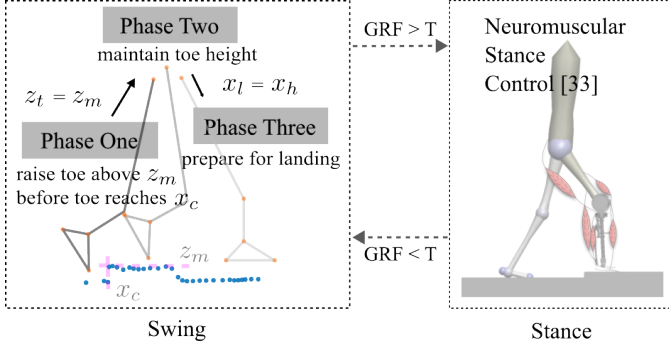


Fig. 4. Prosthesis controller overview. The controller is either in stance or swing phase, depending on the prosthesis leg ground reaction force crossing a threshold T . Stance control uses a virtual neuromuscular model mimicking human leg behavior [33]. Swing control is implemented as detailed in section II and investigated in this paper.

III. PROSTHESIS EXPERIMENTS AND RESULTS

A. Prosthesis Control Implementation

The controller of the active knee and ankle prosthesis is implemented within the Simulink Real-Time environment and operates at a 1 kHz update rate. The prosthesis knee and ankle joints are driven by two separate series elastic actuators, which can be operated in torque or position control. Two IMUs mounted above the knee and on the foot of the prosthesis are used for state estimation. During swing, the prosthesis knee is controlled as detailed in section II (Fig. 4, left panel). Specifically, the resulting knee velocity command (6) is integrated and tracked with position control [34]. The prosthesis ankle joint follows a minimum jerk trajectory that is generated at toe-off and returns the ankle to a perpendicular position. Although the focus of this paper is on swing control, the prosthesis implements a virtual neuromuscular control for both the knee and ankle during stance that mimics human leg behavior in this phase [33] (Fig. 4, right panel).

B. Experiments

We evaluated the effectiveness of the proposed swing control through treadmill locomotion experiments with three non-amputee participants (one female, two male) (Fig. 5). All participants provided written informed consent as per a protocol approved by the University Review Board. The participants used the knee and ankle prosthesis with an able-bodied adapter and engaged in level walking as well as stepping over and onto obstacles while the treadmill operated at a speed of 0.7 m s^{-1} for safety. The obstacles consisted of four cardboard boxes: three with heights of 4 cm, 8 cm, and 16 cm for step-overs and one reinforced 16 cm box for step-ons. During a trial, we randomly selected these four boxes 15 to 20 times and placed them on the belt at the front of the treadmill. Apart from the goal of stepping over or onto the obstacles, we instructed the participants to lightly hold onto the handrails for safety but only support their bodies through the handrails when they felt uncomfortable. We gave no additional guidance. All participants had ample practice walking with the prosthesis, and we conducted the experiments only once they reported feeling comfortable. We recorded at

least three trials per participant and task (level walking and obstacle encounters), which resulted in observing at least 100 walking steps, 50 step-overs, and 10 step-ons per participant. For observing ground truth, we used motion capture at 200 Hz of reflective markers placed on the great trochanter of the participant and the knee, toe and heel of the prosthesis.

C. Results

Across the many steps of walking on level ground and over and onto obstacles of various heights and initial distances from the prosthesis, the control maintained a 100% success rate for all three participants, as long as the camera had the obstacle in its view at the time of take-off. On rare occasions, an obstacle was placed too far away and the control incorrectly assumed level ground, causing the prosthesis toe to strike the obstacle late in the swing phase. Rather than the result of the overall control strategy, these failure instances arose from a specific limitation of the depth camera we used. The camera's field of view is 65° , which limited the distance it could look ahead on the ground to 1 m. This distance was not enough to cover the largest initial distances to the obstacles that occurred.

1) *Environment Awareness*: Environment awareness was critical to raise the foot for obstacle negotiation. Figure 5-b shows three representative examples of the user hip and prosthesis knee trajectories during level walking (top), obstacle step-over (middle) and step-on (bottom). In all three cases, the user hip performed similarly (blue trajectories) in the first 300 ms of swing, suggesting the participants did not actively intervene when the swing control was in phase one and raised the prosthesis foot above the obstacle height. In contrast, to achieve foot clearance, the prosthesis knee flexed significantly more with obstacles present (reaching about 80° peak flexion vs. 60° in level walking). This increased knee flexion is also visible in the video capture still frames at the transition between phases one and two (Fig. 5-c), where the prosthesis foot is clearly above the box as intended.

The findings from the representative examples generalize to all three participants and trials. Figure 6 summarizes the swing trajectories of the prosthesis knee angle and the user hip angle and height observed in the three tasks for all three participants. Again, the user hip angle trajectory remains similar for all three tasks in the first 300 ms of swing (θ_h , middle row), while the prosthesis knee flexes substantially more during obstacle encounters (θ_k , top row). In addition, while subjects A and C elevated their hips in the obstacle tasks more than in the level walking (Δz_h , bottom row), the similarity of the hip height changes between the three tasks for subject B show that this active intervention was not critical.

2) *Human Cooperativeness*: The swing control was effective at including the participants in determining the prosthesis motion during swing. By control design, a user can influence the prosthesis swing motion in three essential ways: speed up or slow down the entire swing as the prosthesis knee motion is synchronized to the user hip angular velocity throughout (Eqs. 1-5); lengthen or shorten the prosthesis step by progressing more or less forward on the contralateral stance leg, as phase two (maintain toe height) of the control

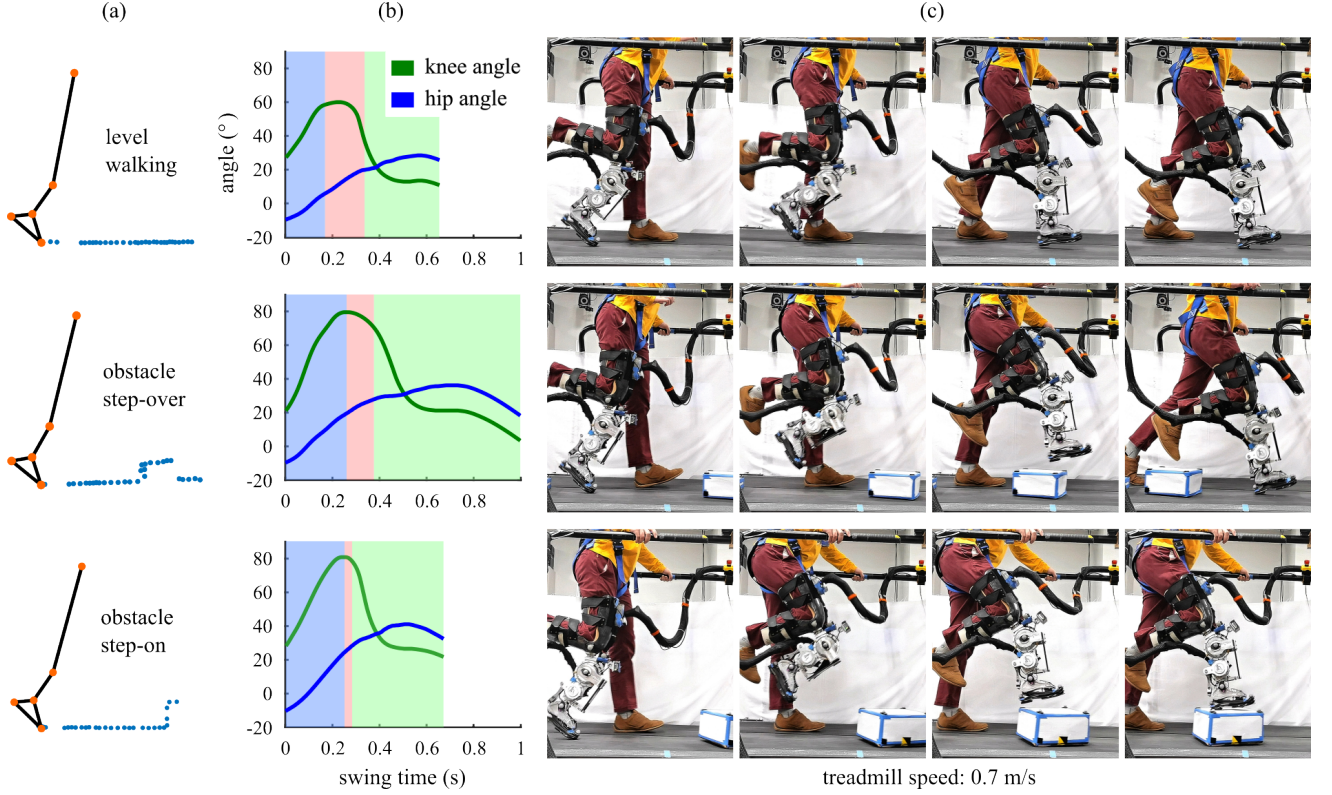


Fig. 5. Representative examples for experimental results in level walking (top), stepping over (middle) and stepping onto (bottom) obstacles. (a) Elevation maps at time of prosthesis leg toe-off. (b) Estimated swing trajectories of user hip angle θ_h (blue) and resulting prosthesis knee angle θ_k (green). Swing control phases (see Sec. II) shaded in light blue, pink, and green for phases one, two and three, respectively. (c) Video capture still frames at toe-off, the transition between phases one and two, the moment the knee angle converges to $\theta_k^t = \theta_h^t - \theta_0$, and at heel-strike.

only transitions to phase three (prepare for landing) once the horizontal position of the prosthesis heel catches up with the user hip ($x_l = x_h$); and effect landing of the prosthesis by extending and lowering the hip in phase three, as the control only locks in a constant forward lean θ_0 of the prosthesis shank without predefining a landing point. The participants used two of these three ways to negotiate the obstacles. They used less hip forward progression (Fig. 5-b, early termination of control phase 2, and Fig. 6, hip forward position Δx_h) to effect shorter steps onto the obstacles and more forward progression combined with delayed landing in phase three to effect larger steps over obstacles (Fig. 5-c, last two still frames, and Fig. 6, average swing time 0.81 s for step-overs vs. 0.64 s for step-ons and 0.61 s for level walking). The participants did not significantly speed up or slow down swing through faster or slower hip angular motion (Fig. 6, middle row), which may be due to the fixed treadmill speed used in the experiments. Overall, the indirect influence on the prosthesis control felt natural to the participants and proved effective at incorporating them in determining the swing motion of the prosthesis.

To further demonstrate the human-cooperativeness of the proposed swing control, figure 7 shows for one participant the foot height trajectories of representative steps during level walking and obstacle encounters. The trajectories demonstrate that the control is effective at providing sufficient foot clearance for various obstacle heights (0 cm to 16 cm), allows the participant to negotiate the obstacles from varying distances

at the onset of swing (70 cm to 15 cm), and enables the participant to effect lowering and thereby determine the landing location for a significant portion of the mid to late swing (Eq. 5 active, solid line portion of trajectories).

IV. DISCUSSION

We presented a novel prosthesis control that adapts the swing motion of a powered lower limb prosthesis to an obstacle in the path while including the human user in determining where and when to land. In validation experiments with three non-amputee participants, we demonstrated the effectiveness of the control when negotiating obstacles of varying sizes and initial distances to the prosthesis as well as when pursuing the competing goals of stepping over or onto the obstacles. To our knowledge, this work is the first to demonstrate real-time control of a lower limb prosthesis that integrates both environment information and user interaction.

Our findings support the claim that environment information is vital for broadening the locomotion activities provided by wearable robots and enhancing their quality of assistance [8]. Without environment information, lower-limb prostheses rely on specific, unnatural motion cues to alter swing and navigate more complex landscapes. For example, commercial knee prostheses like the OttoBock Genium series [35] require the users to extend their hip backwards (contrary to the natural flexion forward) at the beginning of swing to trigger a passive yet rapid flex and extend motion of the prosthesis knee that

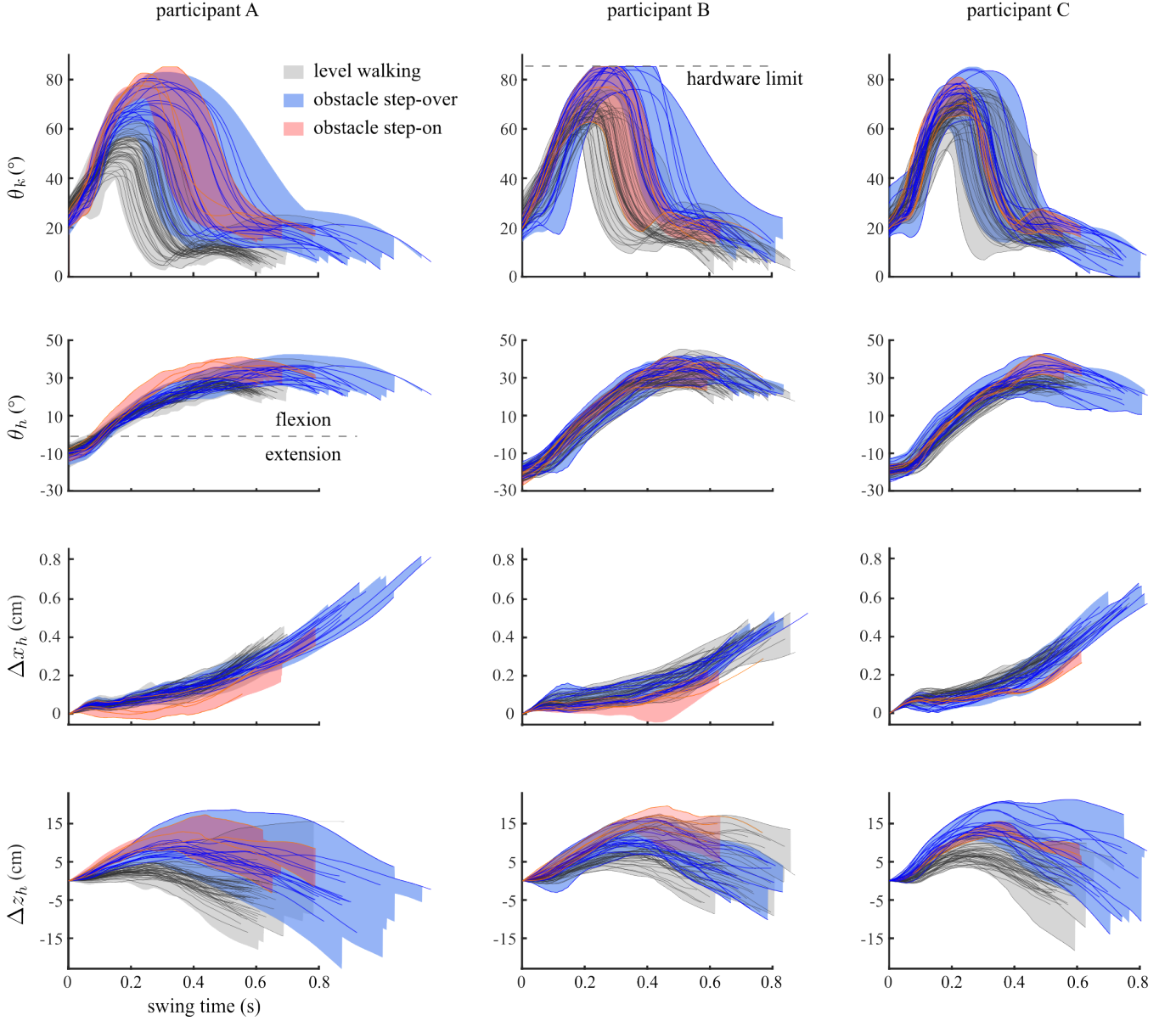


Fig. 6. Swing-phase kinematic trajectories of the three participants for all trials. (Top row) Prosthesis knee angle, (second row) user's hip angle, (third row) hip forward position (relative to take-off), and (bottom row) hip height (relative to take-off) for each participant (columns). Shaded areas indicate the range of trajectories for level walking (gray), and stepping over (blue) and onto obstacles (red), with the areas' upper and lower bounds marking the largest and smallest observed values. The upper bound of the prosthesis knee angle is hardware-limited to 85° . Thin solid lines show randomly selected example trajectories.

enables stair climbing and stepping on and over obstacles. Similarly, control strategies proposed in the research community for powered lower-limb prostheses require unnatural hip extension at the onset of swing to either lock the prosthesis knee [36] or flex it in proportion to the duration of the backward extension [37] to step over obstacles. While effective to an extent, it is unclear how such motion cues may generalize to a wider array of locomotion tasks, such as climbing ladders or rocks. None of these complications seem necessary if environment information becomes integral to prosthesis control. Yet, control strategies that solely rely on environment information [26]–[29] deprive users of agency and, thus, equally restrict the locomotion tasks that can be addressed. On the other hand, our proposed control strategy

leverages environment information to adapt the prosthesis motion to obstacles from early to mid swing while taking advantage of biomechanical cues that naturally occur from mid to late swing (transition from backward to forward lean of the prosthetic leg, lowering and extension of the hip at the end of swing) to let the user shape the prosthesis motion, suggesting how environment information and human interaction may be combined synergistically to enhance the quality of assistance.

Further research will be needed to fully evaluate the potential of the proposed control strategy. First, it has yet to be tested with amputee users. During swing, transfemoral amputees show a reduced hip range of motion in the sagittal plane and hip hiking in the frontal plane when compared to able-bodied walking [38]. The first difference occurs due

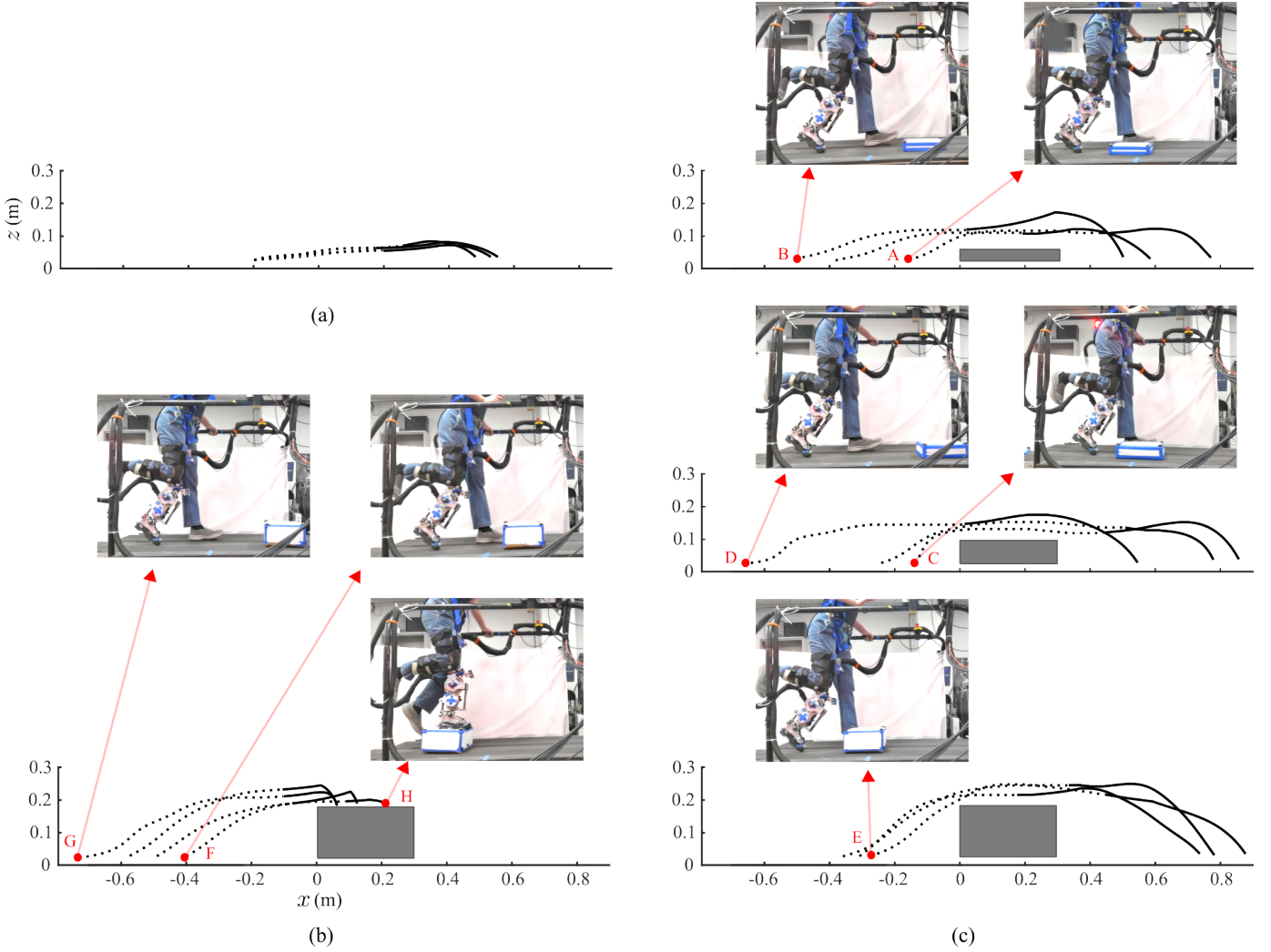


Fig. 7. Example foot height trajectories for participant A in level walking (a), and stepping on (b) and over (c) obstacles. Foot height defined as the lower value of toe and heel heights captured by the motion capture system. The solid line portions mark part of trajectories where swing control applies equation 5 and prosthesis shank maintains constant forward lean θ_0 . Obstacles indicated as gray boxes and x-axis defined relative to point x_c identified from the environment map. Video capture still frames from selected toe-off moments (A-G) and moment after stepping on the obstacle (H) illustrate the variability in obstacle height and initial distance as well as in task that the proposed swing control successfully handles.

to ischium-socket interference [39] and affects hip extension in the early phase of swing while the second difference is believed to compensate for the limited dorsiflexion in commercial prosthetic ankles [40]. Neither of these differences should have a significant impact on the proposed control, as it adapts the prosthesis motion to changes in the user hip angle (Eqs. 1-5) and hip translational motion (region M_z^t changes with hip height and forward progression). However, amputee users may not feel safe using such an adaptive prosthesis control and reject it.

Second, we only demonstrated obstacle negotiation in a confined treadmill locomotion environment, and it remains open whether the control strategy generalizes to other locomotion tasks and realistic environments. Although designed for stepping over and onto obstacles, extending the control to other common locomotion tasks such as negotiating ramps and stairs should be possible, as going up a ramp or stairs resembles stepping onto an obstacle repeatedly and the swing motion during downward steps may be likened to the second half of

the swing motion when stepping over an obstacle. In fact, in preliminary tests we found that the current swing control worked equally well for stepping down from an obstacle as for stepping onto and over it (see supplementary video: [movie S1](#)). On the other hand, the current information we extract from the environment (obstacle height and distance) is clearly insufficient in more varied and realistic environments. For instance, a flight of stairs will have multiple elevations and a human user may want to take one, two or more steps at once. An exciting direction for future research would be to combine our work with work on smart glasses for environment identification [41] and gaze detection [42]. For instance, humans locate future, intended foot placements with a constant look-ahead time [42], which could be used to identify which step of a flight of stairs a user wants to use. In addition, such a transition to smart glasses for extracting environment information (and intent) could also alleviate concerns about the practicality of a prosthesis-bound vision system.

REFERENCES

- [1] F. Sup, H. A. Varol, J. Mitchell, T. J. Withrow, and M. Goldfarb, "Preliminary evaluations of a self-contained anthropomorphic transfemoral prosthesis," *IEEE/ASME Transactions on mechatronics*, vol. 14, no. 6, pp. 667–676, 2009.
- [2] T. Lenzi, L. Hargrove, and J. Sensinger, "Speed-adaptation mechanism: Robotic prostheses can actively regulate joint torque," *IEEE Robotics & Automation Magazine*, vol. 21, no. 4, pp. 94–107, 2014.
- [3] D. Shi, W. Zhang, W. Zhang, and X. Ding, "A review on lower limb rehabilitation exoskeleton robots," *Chinese Journal of Mechanical Engineering*, vol. 32, no. 1, pp. 1–11, 2019.
- [4] S. Hood, S. Creveling, L. Gabert, M. Tran, and T. Lenzi, "Powered knee and ankle prostheses enable natural ambulation on level ground and stairs for individuals with bilateral above-knee amputation: a case study," *Scientific Reports*, vol. 12, no. 1, p. 15465, 2022.
- [5] M. Kim, A. M. Simon, and L. J. Hargrove, "Seamless and intuitive control of a powered prosthetic leg using deep neural network for transfemoral amputees," *Wearable technologies*, vol. 3, p. e24, 2022.
- [6] T. K. Best, C. G. Welker, E. J. Rouse, and R. D. Gregg, "Data-driven variable impedance control of a powered knee–ankle prosthesis for adaptive speed and incline walking," *IEEE Transactions on Robotics*, vol. 39, no. 3, pp. 2151–2169, 2023.
- [7] R. Gehlhar, M. Tucker, A. J. Young, and A. D. Ames, "A review of current state-of-the-art control methods for lower-limb powered prostheses," *Annual Reviews in Control*, vol. 55, pp. 142–164, 2023.
- [8] L. Gionfrida, D. Kim, D. Scaramuzza, D. Farina, and R. D. Howe, "Wearable robots for the real world need vision," *Science Robotics*, vol. 9, no. 90, p. eadj8812, 2024.
- [9] M. Tschiedel, M. F. Russold, and E. Kaniusas, "Relying on more sense for enhancing lower limb prostheses control: a review," *Journal of neuroengineering and rehabilitation*, vol. 17, pp. 1–13, 2020.
- [10] M. Liu, D. Wang, and H. Huang, "Development of an environment-aware locomotion mode recognition system for powered lower limb prostheses," *IEEE Transactions on Neural Systems and Rehabilitation Engineering*, vol. 24, no. 4, pp. 434–443, 2015.
- [11] S. Luo, X. Shu, H. Zhu, and H. Yu, "Early prediction of lower limb prostheses locomotion mode transition based on terrain recognition," *IEEE Sensors Journal*, 2023.
- [12] N. E. Krausz, T. Lenzi, and L. J. Hargrove, "Depth sensing for improved control of lower limb prostheses," *IEEE Transactions on Biomedical Engineering*, vol. 62, no. 11, pp. 2576–2587, 2015.
- [13] Y. Massalin, M. Abdrakmanova, and H. A. Varol, "User-independent intent recognition for lower limb prostheses using depth sensing," *IEEE Transactions on Biomedical Engineering*, vol. 65, no. 8, pp. 1759–1770, 2017.
- [14] K. Zhang, C. Xiong, W. Zhang, H. Liu, D. Lai, Y. Rong, and C. Fu, "Environmental features recognition for lower limb prostheses toward predictive walking," *IEEE transactions on neural systems and rehabilitation engineering*, vol. 27, no. 3, pp. 465–476, 2019.
- [15] K. Karacan, J. T. Meyer, H. I. Bozma, R. Gassert, and E. Samur, "An environment recognition and parameterization system for shared-control of a powered lower-limb exoskeleton," in *2020 8th IEEE RAS/EMBS International Conference for Biomedical Robotics and Biomechatronics (BioRob)*. IEEE, 2020, pp. 623–628.
- [16] N. E. Krausz and L. J. Hargrove, "Sensor fusion of vision, kinetics, and kinematics for forward prediction during walking with a transfemoral prosthesis," *IEEE Transactions on Medical Robotics and Bionics*, vol. 3, no. 3, pp. 813–824, 2021.
- [17] M. Li, B. Zhong, E. Lobaton, and H. Huang, "Fusion of human gaze and machine vision for predicting intended locomotion mode," *IEEE Transactions on Neural Systems and Rehabilitation Engineering*, vol. 30, pp. 1103–1112, 2022.
- [18] M. Ramanathan, L. Luo, J. K. Er, M. J. Foo, C. H. Chiam, L. Li, W. Y. Yau, and W. T. Ang, "Visual environment perception for obstacle detection and crossing of lower-limb exoskeletons," in *2022 IEEE/RSJ International Conference on Intelligent Robots and Systems (IROS)*. IEEE, 2022, pp. 12 267–12 274.
- [19] S. Yin, X. Chen, T. Ma, Y. Wang, Y. Guo, Y. Leng, and C. Fu, "Environmental recognition and multimode continuous-phase control for a powered transfemoral prosthesis," in *2023 IEEE International Conference on Development and Learning (ICDL)*. IEEE, 2023, pp. 55–60.
- [20] B. Zhong, R. L. Da Silva, M. Tran, H. Huang, and E. Lobaton, "Efficient environmental context prediction for lower limb prostheses," *IEEE Transactions on Systems, Man, and Cybernetics: Systems*, vol. 52, no. 6, pp. 3980–3994, 2021.
- [21] V. Rai, D. Boe, and E. Rombokas, "Vision for prosthesis control using unsupervised labeling of training data," in *2020 IEEE-RAS 20th International Conference on Humanoid Robots (Humanoids)*. IEEE, 2021, pp. 326–333.
- [22] B. Laschowski, W. McNally, A. Wong, and J. McPhee, "Environment classification for robotic leg prostheses and exoskeletons using deep convolutional neural networks," *Frontiers in Neurorobotics*, vol. 15, p. 730965, 2022.
- [23] A. G. Kurbis, B. Laschowski, and A. Mihailidis, "Stair recognition for robotic exoskeleton control using computer vision and deep learning," in *2022 International Conference on Rehabilitation Robotics (ICORR)*. IEEE, 2022, pp. 1–6.
- [24] M. A. Contreras-Cruz, L. Novo-Torres, D. J. Villarreal, and J.-P. Ramirez-Paredes, "Convolutional neural network and sensor fusion for obstacle classification in the context of powered prosthetic leg applications," *Computers and Electrical Engineering*, vol. 108, p. 108656, 2023.
- [25] E. Tricomi, M. Mossini, F. Missiroli, N. Lotti, X. Zhang, M. Xiloyannis, L. Roveda, and L. Masia, "Environment-based assistance modulation for a hip exosuit via computer vision," *IEEE Robotics and Automation Letters*, vol. 8, no. 5, pp. 2550–2557, 2023.
- [26] S. Cheng, C. A. Laubscher, and R. D. Gregg, "Automatic stub avoidance for a powered prosthetic leg over stairs and obstacles," *IEEE Transactions on Biomedical Engineering*, 2023.
- [27] Z. Hong, S. Bian, P. Xiong, and Z. Li, "Vision-locomotion coordination control for a powered lower-limb prosthesis using fuzzy-based dynamic movement primitives," *IEEE Transactions on Automation Science and Engineering*, 2023.
- [28] K. Zhang, J. Luo, W. Xiao, W. Zhang, H. Liu, J. Zhu, Z. Lu, Y. Rong, C. W. de Silva, and C. Fu, "A subvision system for enhancing the environmental adaptability of the powered transfemoral prosthesis," *IEEE transactions on cybernetics*, 2020.
- [29] N. Thatte, N. Srinivasan, and H. Geyer, "Real-time reactive trip avoidance for powered transfemoral prostheses," in *Robotics: Science and Systems*, 2019.
- [30] D. Weber and A. Matsiko, "Assistive robotics should seamlessly integrate humans and robots," *Science Robotics*, vol. 8, no. 83, p. eadl0014, 2023.
- [31] A. Likas, N. Vlassis, and J. J. Verbeek, "The global k-means clustering algorithm," *Pattern recognition*, vol. 36, no. 2, pp. 451–461, 2003.
- [32] C. W. Warren, "Global path planning using artificial potential fields," in *1989 IEEE International Conference on Robotics and Automation*. IEEE Computer Society, 1989, pp. 316–317.
- [33] N. Thatte and H. Geyer, "Toward balance recovery with leg prostheses using neuromuscular model control," *IEEE Transactions on Biomedical Engineering*, vol. 63, no. 5, pp. 904–913, 2015.
- [34] N. Thatte, T. Shah, and H. Geyer, "Robust and adaptive lower limb prosthesis stance control via extended kalman filter-based gait phase estimation," *IEEE Robotics and Automation Letters*, vol. 4, no. 4, pp. 3129–3136, 2019.
- [35] M. Bellmann, T. Schmalz, E. Ludwigs, and S. Blumentritt, "Stair ascent with an innovative microprocessor-controlled exoprosthetic knee joint," *Biomedizinische Technik/Biomedical Engineering*, vol. 57, no. 6, pp. 435–444, 2012.
- [36] S. Rezazadeh, D. Quintero, N. Divekar, E. Reznick, L. Gray, and R. D. Gregg, "A phase variable approach for improved rhythmic and non-rhythmic control of a powered knee-ankle prosthesis," *IEEE Access*, vol. 7, pp. 109 840–109 855, 2019.
- [37] J. Mendez, S. Hood, A. Gunnel, and T. Lenzi, "Powered knee and ankle prosthesis with indirect volitional swing control enables level-ground walking and crossing over obstacles," *Science robotics*, vol. 5, no. 44, 2020.
- [38] Y. Sagawa Jr, K. Turcot, S. Armand, A. Thevenon, N. Vuillerme, and E. Watelain, "Biomechanics and physiological parameters during gait in lower-limb amputees: a systematic review," *Gait & posture*, vol. 33, no. 4, pp. 511–526, 2011.
- [39] M. Rabuffetti, M. Recalcati, and M. Ferrarin, "Trans-femoral amputee gait: Socket–pelvis constraints and compensation strategies," *Prosthetics and orthotics international*, vol. 29, no. 2, pp. 183–192, 2005.
- [40] P.-F. Su, S. A. Gard, R. D. Lipschutz, and T. A. Kuiken, "Gait characteristics of persons with bilateral transtibial amputations," *Journal of rehabilitation research & development*, vol. 44, no. 4, 2007.
- [41] D. Rossos, A. Mihailidis, and B. Laschowski, "Ai-powered smart glasses for sensing and recognition of human-robot walking environments," in *2024 10th IEEE RAS/EMBS International Conference for Biomedical Robotics and Biomechatronics (BioRob)*. IEEE, 2024, pp. 62–67.

- [42] J. S. Matthis, J. L. Yates, and M. M. Hayhoe, “Gaze and the control of foot placement when walking in natural terrain,” Current Biology, vol. 28, no. 8, pp. 1224–1233, 2018.